INTERNATIONAL JOURNAL OF CLIMATOLOGY, VOL. 15, 187–205 (1995) 551.577.38:551.583.4(64)

SPATIO-TEMPORAL PATTERNS OF DROUGHT IN MOROCCO

NABIL CHBOUKI

Department of Forestry, Institute of Agronomy and Veterinary Medicine, BP 6202, Rabat-Instituts, Rabat, Morocco

CHARLES W. STOCKTON

Laboratory of Tree-Ring Research, University of Arizona. Special Consultant To King Hassan II of Morocco, Direction de la Recherche et Planification de l'Eau, Administration de l'Hydraulique, Rue Hassan Benchekroun, Agdal, Rabat, Morocco

AND

DONALD E. MYERS

Department of Mathematics, University of Arizona, Tucson, Arizona 85721, USA

Received 15 January 1993
Accepted 24 March 1994

ABSTRACT

Past climatic moisture anomalies can be reconstructed from climatically sensitive tree-ring chronologies of *Cedrus atlantica* in Morocco. A map-pattern technique was utilized to derive 10 patterns of variability for the period 1845–1974. The individual patterns were examined, in space using geostatistical techniques, and in time using correlation coefficients. The results indicate a clear alternation of favourable-unfavourable climatic regimes lasting 20–25 years. The spatial extent of the climatic moisture anomalies can be explained by a combination of three factors of the atmospheric circulation related to the Azores High, local cyclogenesis, and north-eastern perturbations.

KEY WORDS: tree rings; map pattern; drought; variograms; kriging; pressure types; Morocco

INTRODUCTION

Drought is a common climatic anomaly in Morocco, which may have very harmful consequences. It is necessary to better understand its characteristics and establish its history from long-living and sensitive trees of *Cedrus atlantica* (Stockton, 1985; Chbouki, 1992). Temporal occurrences of drought are perceived based on their spatial characteristics and the regional losses they induce. In order to characterize past droughts, both their spatial and temporal behaviour should be addressed. Recurrence intervals, frequency, duration, severity, and areal extent are space–time characteristics to be derived. A simultaneous analysis is desirable but is often difficult to implement and interpret. This is the case with space–time geostatistics. To describe spatio-temporal variability, three- (or higher) dimensional variograms are computed and modelled (Rouhani and Hall, 1989). However, as stated by Rouhani and Myers (1990), extension of geostatistical techniques to the space–time domain raises difficulties stemming from the differential nature and amount of spatial (few locations) versus temporal (long series) data.

An alternative approach would be to summarize variability in one domain and study it in the other domain. Whether to start with space or time is of particular relevance because the two methods address different questions. A summary of spatial variability is identical to clustering, which would identify homogeneous regions or spatial ranges of variability. However, no explicit identification of dry events is made. On the other hand, summarizing temporal variability will lead to identification of drought types that can then be examined in space. This approach is more appropriate to the present investigation and will be followed here.

CCC 0899-8418/95/020187–19

DATA

The area of study forms a regular 30 × 40 block grid of 10 km × 10 km cells extending from 400 km to 700 km longitude and 150 km to 550 km latitude and covering most of northern Morocco. The coordinates are given in the Lambert system. Precipitation-sensitive dendrochronological series are used to reconstruct past occurrences of drought (Meko, 1985; Stockton, 1985; Till, 1985). The tree-ring data base was compiled from a Belgian collection by Munaut, the Laboratory of Tree-Ring Research collection of the University of Arizona by Stockton, and our own collection. It includes 48 sites covering the whole natural habitats of *Cedrus atlantica* in Morocco (Figure 1). The scatter of sites reflects the spatial extent and distribution of the Atlas Cedar forests in Morocco. They form four distinct zones in the Rif, the central Middle Atlas, the oriental Middle Atlas, and the oriental High Atlas. A site refers to a localized geographical area (of few hundred square metres) with homogeneous ecological conditions.

The Atlas Cedar tree rings exhibit a sharp transition between late wood of the $year_{t-1}$ (dark band with small cells and thick walls) and early wood of the $year_t$ (light coloured band with larger cells and thin walls). These anatomical features are used to date the cores.

At least 10 trees were cored per site, with two cores per tree. The individual cores have been cross-dated to account for missing or double rings, the dates statistically checked, and then the series standardized to remove age trends and other non-climatic signals (Stokes and Smiley, 1968; Homes *et al.*, 1986; Cook, 1987). Cores that cross-dated poorly were omitted, but overall, the sample depths for mean chronologies were satisfactory (Chbouki, 1992). The final series correspond to unitless indices retaining a strong climatic signal. In fact, correlation analyses show good relationships between tree-ring data and precipitation data over the whole area of study (Chbouki, 1992). Table I summarizes the tree-ring statistics. The data analysis has been carried out for the common period 1845–1974 (130 years).

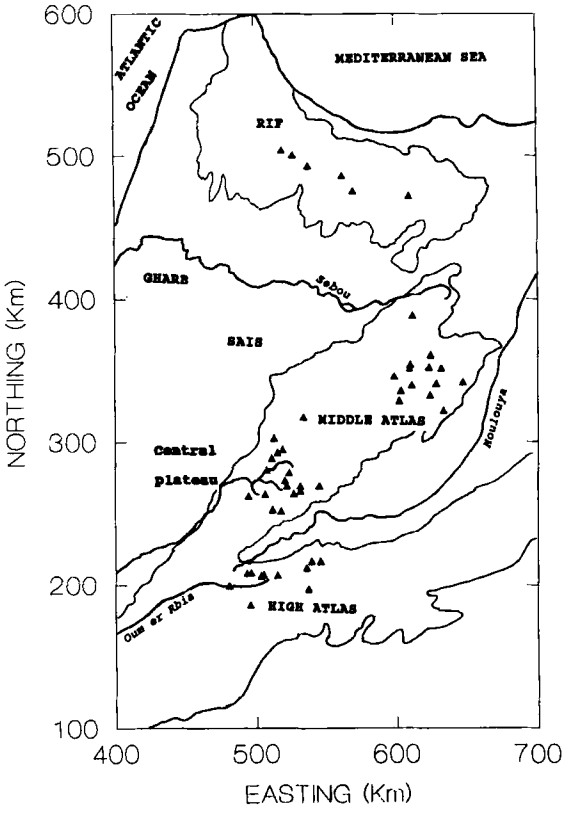

Figure 1. Location of the tree-ring sites within the study area

Table I. ARSTAN chronology statistics

Site number	MSEN	SD	SER1	SER2	S/N	SK	KUR
01	0·150	0·172	0·393	−0·102	6·751	−0·396	2·958
02	0·149	0·200	0·580	0·200	2·355	−0·441	2·187
03	0·196	0·203	0·282	−0·214	6·698	−0·603	1·461
04	0·227	0·267	0·523	0·096	9·896	−0·342	0·981
05	0·144	0·163	0·426	−0·015	5·981	−0·089	0·513
06	0·147	0·177	0·373	0·016	2·791	0·807	1·792
07	0·355	0·331	0·444	0·324	5·275	−0·984	1·164
08	0·319	0·328	0·372	0·150	9·840	−0·008	0·187
09	0·349	0·395	0·437	0·237	2·232	0·511	2·672
10	0·376	0·381	0·381	0·206	16·239	0·151	0·486
11	0·418	0·356	0·122	0·110	15·586	−0·240	0·142
12	0·330	0·339	0·331	0·191	14·814	−0·125	−0·126
13	0·376	0·376	0·349	0·179	29·057	−0·105	−0·214
14	0·462	0·436	0·321	0·202	16·086	−0·027	−0·237
15	0·304	0·322	0·441	0·120	16·926	−0·270	−0·084
16	0·386	0·411	0·439	0·175	19·517	−0·066	−0·344
17	0·213	0·212	0·236	0·076	10·414	−1·18	2·662
18	0·295	0·295	0·346	0·164	18·207	−0·654	0·914
19	0·175	0·227	0·575	−0·154	3·364	−0·422	0·071
20	0·178	0·242	0·547	0·043	1·817	0·405	3·244
21	0·253	0·289	0·452	0·171	14·984	−0·177	0·582
22	0·373	0·371	0·406	0·182	15·983	−0·226	0·004
23	0·245	0·311	0·591	0·163	2·729	−0·248	0·365
24	0·269	0·301	0·389	0·084	13·720	0·202	1·265
25	0·251	0·292	0·473	0·063	11·354	−0·182	0·467
26	0·135	0·156	0·367	−0·165	6·370	−0·734	1·452
27	0·277	0·304	0·402	0·144	4·245	0·091	1·635
28	0·169	0·186	0·333	0·133	9·338	−0·111	1·004
29	0·223	0·274	0·545	0·087	6·611	−0·228	0·683
30	0·185	0·225	0·503	−0·105	6·271	−1·07	1·583
31	0·153	0·207	0·596	−0·021	6·013	−0·733	1·969
32	0·304	0·343	0·469	0·161	6·079	−0·131	0·421
33	0·207	0·252	0·504	−0·029	7·761	−0·378	0·813
34	0·202	0·245	0·479	0·127	6·157	−0·353	2·113
35	0·199	0·296	0·689	0·010	9·197	−0·561	0·058
36	0·244	0·309	0·593	−0·076	7·886	−0·085	−0·081
37	0·237	0·297	0·557	−0·248	11·973	−0·647	1·084
38	0·185	0·234	0·526	−0·128	3·102	−0·175	0·671
39	0·157	0·175	0·379	−0·003	9·929	0·079	0·343
40	0·155	0·216	0·599	−0·159	7·150	−0·603	0·701
41	0·217	0·278	0·554	0·079	15·931	0·040	0·363
42	0·291	0·361	0·597	0·044	15·933	0·145	0·855
43	0·196	0·301	0·749	0·017	19·298	−0·529	0·492
44	0·267	0·347	0·554	0·108	12·366	0·159	1·298
45	0·247	0·286	0·424	0·072	1·133	−0·057	0·753
46	0·193	0·248	0·567	−0·005	9·812	−0·121	0·455
47	0·162	0·161	0·228	−0·085	1·985	−0·548	2·076
48	0·176	0·269	0·649	0·117	8·717	−0·173	0·692

MSEN = mean sensitivity; SD = standard deviation; SER1/2 = rank 1/2 serial autocorrelation; S/N = signal-to-noise ratio; SK = skewness; KUR = kurtosis.

METHODS

Principal component or correspondence analyses (Greenacre, 1984; Legendre and Legendre, 1984; Johnson and Wichern, 1988) can be used to summarize the temporal or spatial variability in the *Q*-mode or *R*-mode (with time corresponding to the rows of the matrix) on a reduced space. Their use, however, creates two major difficulties. First the patterns obtained may be impossible to interpret. Second, they may have no physical basis, being simply mathematical artefacts due to the stringent orthogonality constraint. For these reasons, many investigators retain only the first few axes that explain most of the variance. An equivalent technique, known as map-pattern analysis, was first developed by Lund (1963; in Fritts, 1976) and refined by Blasing (1975). It aims at identifying climatic moisture anomalies. The procedure consists of computing interannual correlations based on spatial data points, which in this context correspond to tree-ring sites. The tree-ring data are normalized by subtracting the mean and dividing by the standard deviation of the series. Correlations are computed for every year of the period covered by the tree-ring series ($n = 130$ years). Correlation is used as the measure of similarity between the yearly patterns. Once the $n \times n$ correlation matrix is obtained, the procedure selects the year (called index year) that has the highest correlation with the maximum number of years. That year then serves to define the first anomaly type. In the approach used here, the four highest correlated years are averaged along with the index year to form the anomaly type. The averaging removes noise peculiar to a given year and enhances the commonality. Yearly correlations with the anomaly type are then recomputed. The most significant years are assigned to the type and the base years removed from the matrix. The procedure is repeated on the rest of the years, using a lower significance level at each step until it drops below some predetermined cut-off value.

For every anomaly type, the method specifies the years forming the type, the years positively associated with it, and also the ones that are negatively associated with it. Those showing negative associations may form a type by themselves. The method builds on the positive correlations and does not mix opposite signs of the pattern, as is the case with eigenvectors (with principal component analysis (PCA) the eigenvectors express both the positive and the negative modes of a pattern, which may not reflect reality (Blasing, 1975; Fritts, 1976)).

The number of years included in the type average needs to be large enough to screen out the noise and small enough to preserve the specificities of the anomaly type. Five years were chosen, following the work of Oladipo (1985) and Blasing (1975). The analysis identified 10 anomaly types, which have relatively high correlations and distinct temporal patterns. With additional anomaly types, correlations become low and a large number of years are associated, positively or negatively, with the anomaly.

The spatial extent of moisture anomalies was analysed using geostatistics (Matheron, 1971; Journel and Huijbregts, 1978; Isaaks and Srivastava, 1989). First, variography was used to examine and model spatial variability. Second, ordinary block kriging was used to produce the spatial patterns of moisture anomalies. The variogram $\gamma(h)$, being a function of interpoint distance h, was used to describe and quantify the underlying spatial structure. If the phenomenon exhibited a finite variance then $\gamma(h) = C(0) - C(h)$, where $C(h)$ is the covariance. Sample estimator of the variogram is given by

$$\gamma^*(h) = \frac{1}{2N(h)} \sum [Z(x_i + h) - Z(x_i)]^2$$

$N(h)$ is the number of pairs a distance h apart and $Z(x_i)$ the realization of the regionalized variable at the sample site x_i. The optimal sampling pattern is the one that gives large $N(h)$ at short distances. With an irregular data set, distance classes (δh) and tolerance angles ($\delta\theta$) are defined to increase $N(h)$ and improve the estimation. A theoretical model is fitted visually to the sample variogram. The modelling process can take into consideration the presence of a nugget component, which corresponds to a microstructure or to location or random measurement errors. In addition, the modelling searches for possible anisotropic behaviour as revealed by directional sample variograms. Anisotropy indicates whether the spatial phenomenon has preferential directional variations. The model can be given as a positive linear combination

of valid models to account for nested structures. To ensure a robust estimation of the variogram only distances less than half the maximum interpoint distance are used with at least 30 pairs (Journel and Huijbregts, 1978). The final choice of the model is also based on cross-validation using the technique of jack-knifing (Myers, 1991).

Kriging is then used to produce estimates at the unsampled locations of interest, allowing us to establish the spatial extent of climatic moisture anomalies and examine the regional gradients and differences. The estimation may be over a point x_0, a volume or block v_0, or even over the whole area of study D. Kriging uses an optimal linear combination of the available data, given as:

$$Z^*(x_0) = \sum \lambda_i Z(x_i)$$

Optimality is regarded with respect to (i) unbiasedness, and (ii) minimal variance of the estimation error. The weights, λ_i, assigned to the data samples are chosen to attain the optimality conditions.

$$E[Z^*(x_0)] = E[\textstyle\sum \leftarrow_i Z(x_i)] = \sum \lambda_i m = m \sum \lambda_i = m \text{ if } \sum \lambda_i = 1.$$

with m the constant mean of Z. Minimizing the variance of the errors subject to the constraint shown above, a Lagrange multiplier -2μ is introduced and the following expression is minimized:

$$\text{Var}[Z^*(x_0) - Z(x_0)] - 2\mu(\textstyle\sum \lambda_i - 1)$$

being equal to:

$$-\sum\sum \lambda_i \lambda_i \gamma_{ij} + 2 \sum \lambda_j \gamma_{0j} - 2\mu(\textstyle\sum \lambda_i - 1)$$

with γ_{ij} being equal to $\gamma(x_i - x_j)$. Taking the partial derivatives with respect to the λ_is leads to a set of $n+1$ linear equations in $n+1$ unknowns. We obtain the kriging system:

$$\sum \lambda_i \gamma_{ij} + \mu = \gamma_{i0} \qquad i = 1, \ldots, n$$
$$\sum \lambda_i = 1$$

In matrix form, the kriging system is written as:

$$[\mathbf{K}] \times [\lambda] = [\mathbf{M2}] \rightarrow [\lambda] = [\mathbf{K}]^{-1}[\mathbf{M2}]$$

with

$$[\lambda] = \begin{bmatrix} \lambda_1 \\ \vdots \\ \lambda_n \\ \mu \end{bmatrix}, \quad [\mathbf{M2}] = \begin{bmatrix} \lambda_{01} \\ \vdots \\ \lambda_{0n} \\ 1 \end{bmatrix}, \text{ and } [\mathbf{K}] = \begin{bmatrix} \lambda_{11} & \cdots & \lambda_{1n} & 1 \\ \vdots & \cdots & \vdots & \vdots \\ \lambda_{n1} & \cdots & \gamma_{nn} & 1 \\ 1 & \cdots & 1 & 0 \end{bmatrix}$$

The minimum estimation variance, called the kriging variance, is:

$$\sigma_{k2} = \sum \lambda_i \gamma_{i0} + \mu$$

for punctual kriging;

$$\sigma_{k2} = \sum \lambda_i \gamma_{i0} + \mu - \bar{\gamma}(V, V)$$

for block kriging with

$$\bar{\gamma}(V, V) = 1/V^2 \iint \gamma(x - y)\, dx\, dy$$

Compared with other estimation techniques, kriging presents several advantages. The use of a valid variogram model guarantees the existence and uniqueness of the solution. It is an exact interpolator and makes efficient use of the data by screening and declustering them. Finally, for a given location, kriging gives the best linear unbiased estimator (BLUE) and also produces a kriging variance indicating the reliability of the result. A detailed presentation is found in Matheron (1971), Delhomme (1976), Journel and Huijbregts (1978), Clark (1979), and Isaaks and Srivastava (1989).

RESULTS AND DISCUSSION

The technique identified 10 patterns that can be classified as dry or wet. The assignment is based on the correlation of the type, with 1945 taken as a reference dry year and 1963 taken as a reference wet year. Patterns showing a predominant deficit over much of the sites were classified as dry also. The deficits are computed as departures from the mean of the tree-ring series. The anomaly types along with the associated years are given in Table II.

Variography

Sample variograms were computed in four directions in order to detect possible anisotropies. Mean sample variograms were also computed using all pairs available (Figure 2(a)). The Geo-EAS package has been used to carry out the calculations and modelling (EPA, 1988).

Some of the anomaly types have noisy variogram estimates that reveal very little spatial structure. It is assumed that the homogeneity observed induces this noisy pattern resembling a pure nugget effect. This is especially true with severe drought types (types IV and V). Most of the anomalies, however, show a well-structured variability (Figure 2(b)). A pseudo-periodic behaviour is apparent in all of the variograms, which, owing to the geometrical setting of the sites, is considered a reflection of the scatter of sample sites. For some anomaly types it was necessary to rely on directional variograms to discern any pattern of variability (types IV, V, and VII). The estimates do not indicate any anisotropic behaviour and when compared with the pure nuggest effect the noisy models were consistently better. The well-defined structures were easily modelled, whereas the others could not be improved. The final models retained are given in Table III.

The models resemble those that were obtained by Chbouki (1992) for drought attributes in Morocco. However, here the nugget effect is very small, representing a maximum of 25 per cent of structured variability. The ranges vary between 30 km and 50 km, except for types 3 and 6, which show a 70-km range. The models reveal similar generating processes of spatial variation, as did the drought attributes, where local factors dominate. The spherical scheme is the only one used and in all cases was preferable to the exponential one. Directional variography proved difficult, with noisy estimates, and a strong pseudo-periodic behaviour

Table II. Anomaly types

Type code	Base years	Positive associations	Negative associations
1W	1857, 1963, 1856, 1964, 1858	1856–1858, 1963–1965	1850, 1874, 1883
2N	1954, 1955, 1953, 1961, 1890	1889–1890, 1953, 1955, 1961–1962	
3W	1960, 1959, 1958, 1917, 1901	1901, 1904, 1917, 1918, 1956, 1958–1962	1874, 1881, 1883, 1938
4D	1950, 1862, 1951, 1952, 1949	1862, 1949–1952	
5D	1966, 1945, 1968, 1926, 1881	1867–1869, 1874, 1881, 1883, 1884, 1926, 1945, 1966, 1968	1901, 1917, 1956, 1962, 1963
6D	1974, 1948, 1877, 1876, 1973	1869, 1871, 1873, 1874, 1876, 1877, 1881, 1883, 1899, 1926, 1931, 1948, 1973, 1974	1857, 1858, 1901, 1906, 1908, 1917, 1918, 1959–1963
7D	1972, 1971, 1892, 1893, 1933,	1850, 1892, 1893, 1931, 1939, 1971–1973	1858, 1860, 1870, 1927, 1953–1955, 1963–1965, 1967
8D	1947, 1946, 1944, 1897, 1936	1867, 1877, 1883, 1898, 1899, 1926, 1931, 1936, 1937, 1944, 1946–1948	1857, 1858, 1865, 1867, 1894, 1901, 1902, 1904, 1913, 1914, 1957, 1959, 1961, 1965, 1971
9W	1969, 1970, 1942, 1920, 1941	1856, 1893, 1894, 1920, 1921, 1941–1943, 1969, 1970	1849, 1913, 1949 1950, 1953, 1954, 1958, 1959, 1961
10D	1967, 1905, 1925, 1910, 1927	1905, 1907–1912, 1925, 1927, 1965–1968	1853, 1871, 1872, 197, 1898, 1931, 1933, 1934, 1936, 1937, 1948, 1949

W = wet; N = normal; D = dry.

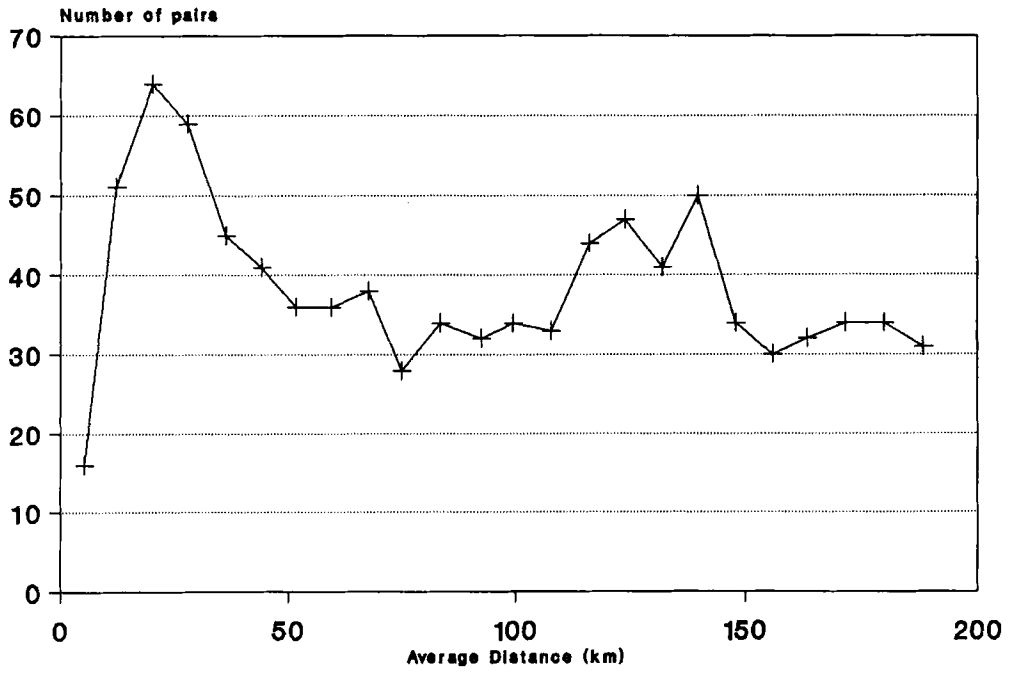

Figure 2. (a) Number of pairs used to estimate the variogram at different lag distances.

was overwhelming and reflected back on the quality of the models. The drought attributes variogram models obtained by Chbouki (1992) could be used to improve the modelling and the estimation processes using cross-variograms, but with 136 pairs of variables the operation would be very time consuming in terms of cross-variogram modelling and computer time.

Kriging

The patterns obtained reveal some interesting contrasts and spatial distributions. Their reliability is very similar. In fact the kriging errors show the same spatial distribution and magnitude despite the differences of their structured variability (Figure 3). They constitute a faithful image of the sample data clustering. The lowest values, or equivalently the most reliable estimates, are found within the four clusters of tree-ring sites. Away from the Atlas Cedar forests, the errors increase as a result of the extension to the unsampled regions.

The following presentation of the anomalies will link them to the pressure types published by the Direction de la Meteorologie Nationale (1990) in order to give a tentative explanation of the atmospheric dynamics creating them.

Anomaly type I

This anomaly corresponds to above average moisture (wetness) over much of the study area. A clear north–south gradient is evident. The wetness is greatest in the south (about one-third of the study area), average over the middle and slightly less than average over the northern third of the domain (Figure 4(a)). This arrangement may be due to particular atmospheric dynamics resulting from meridional migration or shifting of the pressure action centres, with Morocco being at the centre of the perturbations and not at the margin (pressure type IX in Figure 5). This type is very time specific, having occurred during the years 1856–1858 and 1963–1965. The time series of annual correlations with the anomaly shows a clear periodic behaviour (Figure 6). From 1860 to 1900 the association is constantly negative, suggesting the predominance of other types associated with unfavourable conditions. The well-known humid period, 1900–1920, and the

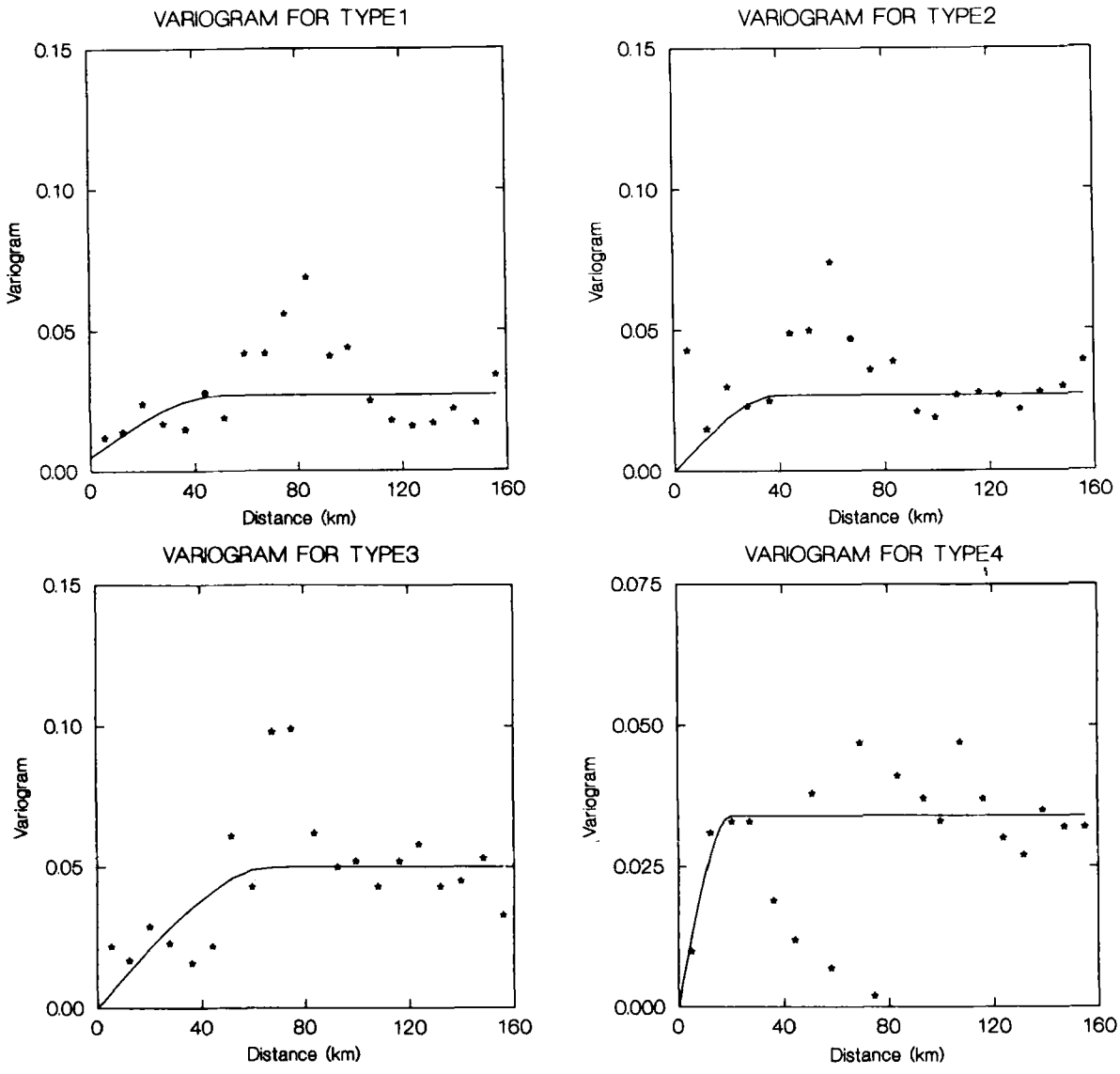

Figure 2. (b) Sample variogram estimates for the anomaly types

Table III. Variogram models for the anomaly types

Types	Model	Nugget	Sill	Range	Percentage SV
1	Spherical	0·005	0·022	50	81·5
2	Spherical	0·000	0·027	40	100·0
3	Spherical	0·000	0·050	70	100·0
4	Spherical	0·000	0·034	20	100·0
5	Spherical	0·010	0·040	30	80·0
6	Spherical	0·006	0·020	70	76·9
7	Spherical	0·000	0·030	40	100·0
8	Spherical	0·005	0·030	40	85·7
9	Spherical	0·005	0·019	35	79·2
10	Spherical	0·000	0·030	40	100·0

SV is the structured variation defined as the sill/nugget ratio.

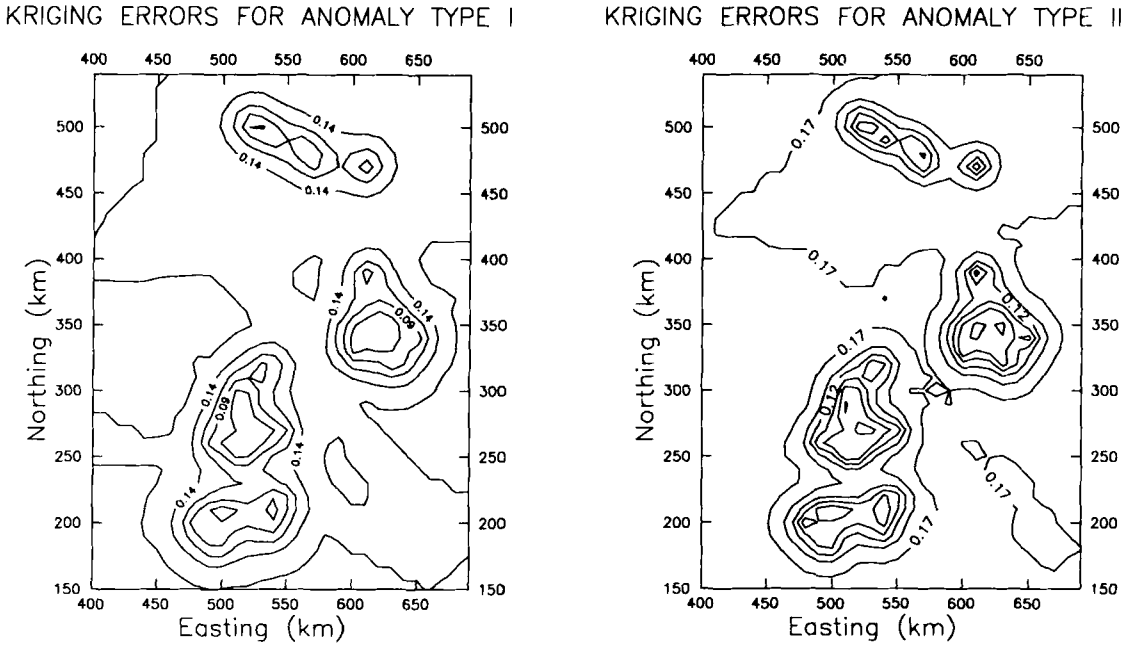

Figure 3. Kriging errors associated with the anomaly types

period in the mid-1960s are consistently positively associated with this anomaly type. The 1970s are negatively associated with this type.

Anomaly type II

This type cannot be classified clearly as dry or wet. For this type, the central Middle Atlas shows a severe moisture deficit and the shortage extends to the central area, forming a band. The Rif experiences only slight moisture increases on its occidental side, whereas the western part of the High Atlas experiences moist conditions (Figure 4(b)). It would be interesting to study the atmospheric circulation types associated with the base years 1953–1955 and 1961 to determine the cause of this localized deficit right in the centre of the country. The annual association with this type was consistently weak until the late 1930s, when they became negative for 20 years (Figure 6). In the 1950s the associations became positive and lasted for about 20 years. The 1970s are markedly negatively associated with this type.

Anomaly type III

This anomaly shows the western part of the study domain experiencing drought, with severe deficits in the central Middle Atlas (Figure 7(a)). The anomaly over the Central Plateau, a remote area with the highest kriging errors, is to be placed into the larger and more reliable spatial context of the western part and should be considered as a moderate deficit. On the oriental side the conditions are about normal or slightly favourable. The High Atlas shows a significant positive moisture anomaly. This can happen if the major atmospheric perturbations are from the south-west, south of the High Atlas, i.e. predominance of pressure types V and VI (Figure 5). The occurrence of this type of atmospheric circulation has a distinct periodic behaviour (Figure 6). The best associations occur during the period 1950–1970 (with a peak at 1960) and during the period 1900–1920. The periods 1860–1890 and 1920–1950 are consistently negatively associated with this pattern.

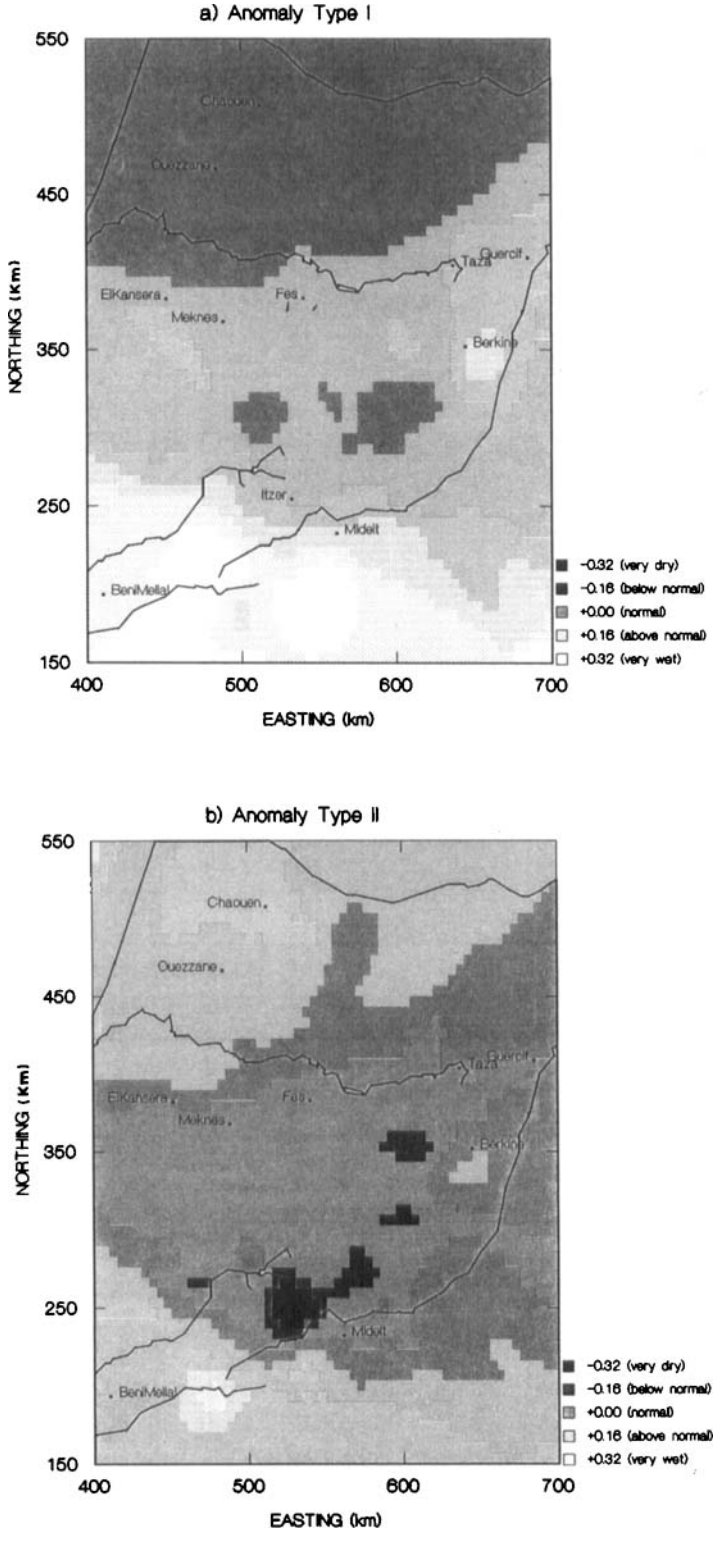

Figure 4. Anomaly types I and II as defined by ordinary block kriging. The shading numbers correspond to the standardized deviations of the tree-ring indices, with negative values for drought and positive values for wetness. The values chosen indicate five severity classes and exhibit good spatial contrast

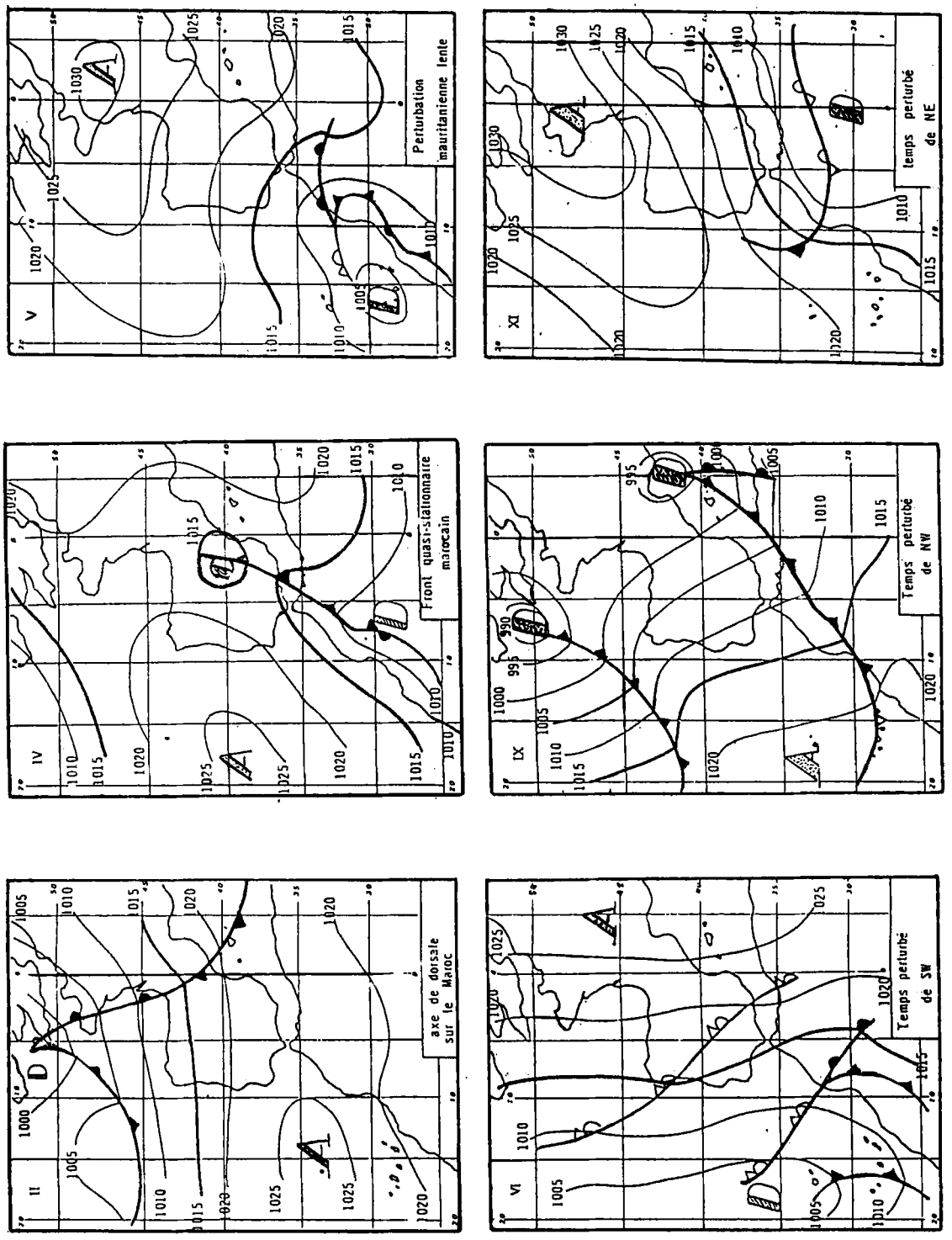

Figure 5. Pressure types over Morocco (after the direction de la Meteorologie Nationale, 1990)

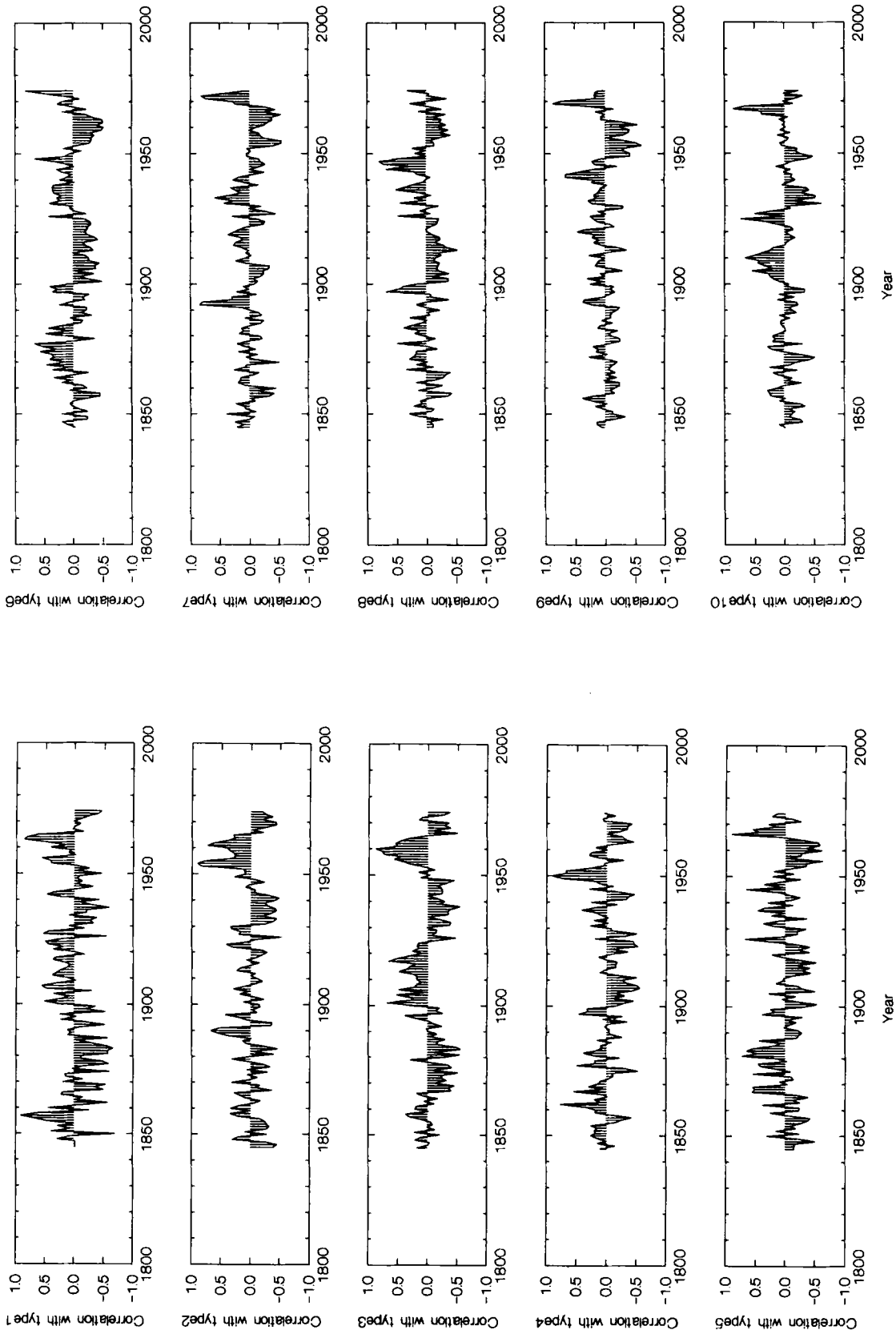

Figure 6. The temporal association with the anomaly types. An anomaly predominates when it shows high yearly positive correlations

Anomaly type IV

Anomaly type IV is a definite drought type (Figure 7(b)). The lower one-third and eastern half of the study area show extreme drought. The rest of the domain is average to slightly dry except for a localized area in the western High Atlas, which exhibits slightly favourable conditions. Once again, the Rif area does not experience the extended deficit. This type can be seen as a mirror image of the wet anomaly type I. It

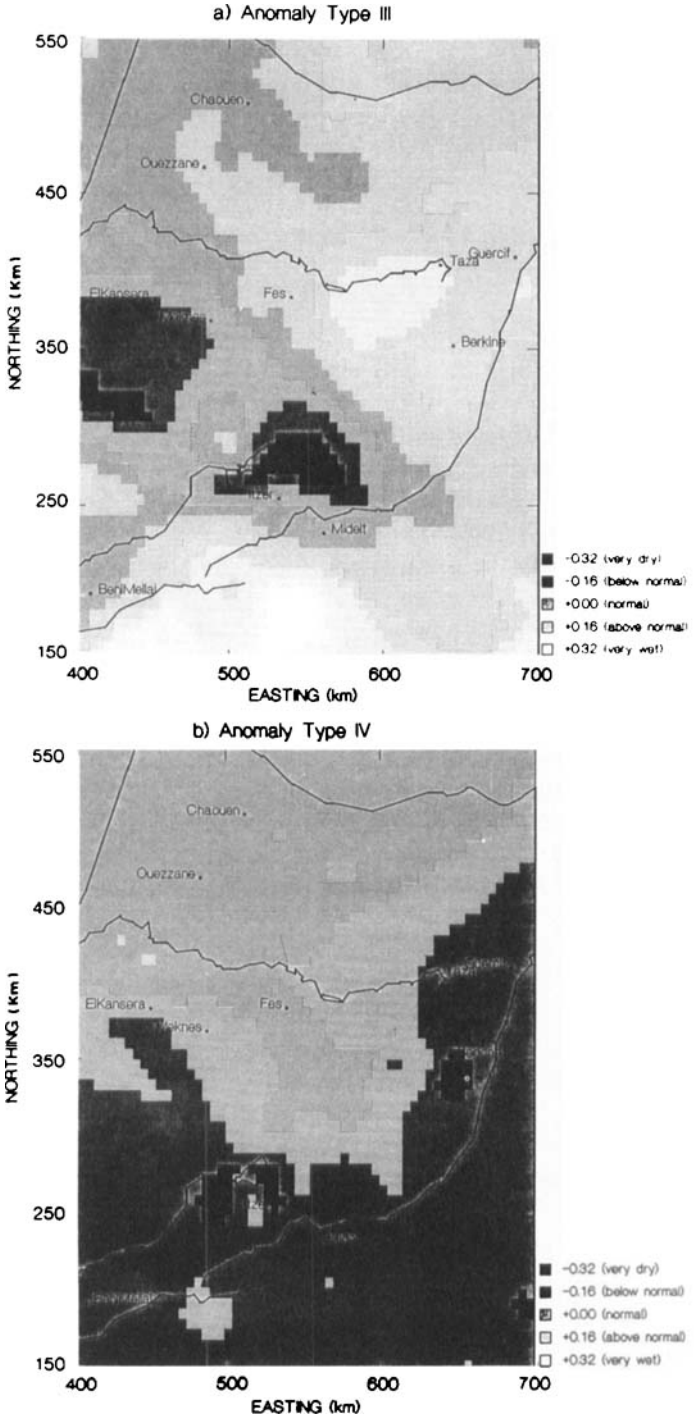

Figure 7. Anomaly types III and IV as defined by ordinary block kriging. See Fig. 4 for explanation

suggests that the storm tracks are located north of the country with the perturbations marginally reaching northern Morocco (pressure type II in Figure 5). This would result if the Azores High is located at a slightly higher latitudinal position. Anomaly type IV occurred frequently in the 1950s and the wet period 1900–1920 is mostly negatively associated with it (Figure 6).

Anomaly type V

Severe and widespread droughts form this anomaly type (Figure 8(a)). The Rif is about normal whereas the eastern part of the country has the worst deficits. In terms of the atmospheric circulation, this type can be seen as an extreme case of the anomaly type IV, with a net blocking effect by the Azores High due to a north-east movement. The period 1870–1890 is well associated with the anomaly (Figure 6). As we have seen with the previous anomalies, the period 1860–1890 was an unfavourable one, because types IV and V prevailed. The wet episode from 1900 to 1920 is negatively associated with them. This type predominated in the period from the mid-1960s to mid-1970s.

Anomaly type VI

In this anomaly type, the region of Taza in the Middle Atlas along with the High Atlas show severe droughts, whereas most of the other parts of the area exhibit a less severe conditions. The rich plains of the Sais and the Gharb are spared drought in this anomaly (Figure 8(b)). One logical explanation of this type, based on the atmospheric circulation capable of producing such spatial variability, is local cyclogenesis taking place in the Atlantic region. This type of perturbation is called Mauritanian (pressure type V in Figure 5), and occurred during the dry episodes, i.e. 1860–1890, 1920–1950, and the 1970s (Figure 6). The anomaly is negatively associated with the wet periods of 1900–1920 and 1950–1965.

Anomaly type VII

This is also a drought type that severely affects the Rif, the Atlantic region and the High Atlas. The eastern regions in general experience normal conditions (Figure 9(a)). The atmospheric dynamics behind this pattern can be summarized by two points. First, the Azores High must be strong and be displaced eastward toward Morocco, where it forms a persistent blocking action diverting all low-pressure systems northward. Second, the eastern regions come under the influence of the Mediterranean Sea, from which they receive moisture through eastern perturbations (pressure type XI in Figure 5). This kind of circulation prevailed during the 1890s and 1970s. From 1950 to 1970 a clear negative association with this type is seen (Figure 6).

Anomaly type VIII

This anomaly type represents the case of moderate droughts localized in the High Atlas and the eastern portion of the study area. The major deficits cover the eastern side of the area (Figure 9(b)). Once again, the central regions of the Gharb, the Sais, and the Central Plateau show above normal conditions. This type resembles that of the anomaly type VI but is less intense. The yearly correlation coefficients present the same temporal pattern, being positive during the same dry episodes and negative during the wet ones (Figure 6).

Anomaly type IX

This type (Figure 10(a)) is the opposite of anomaly type II. It is evident not only in the spatial pattern but also in the yearly correlation coefficients temporal pattern (Figure 6). The central regions have above normal conditions whereas the north and the south show normal to below normal conditions. This pattern is localized in time and manifested after 1940, with a peak in the 1970s (Figure 6).

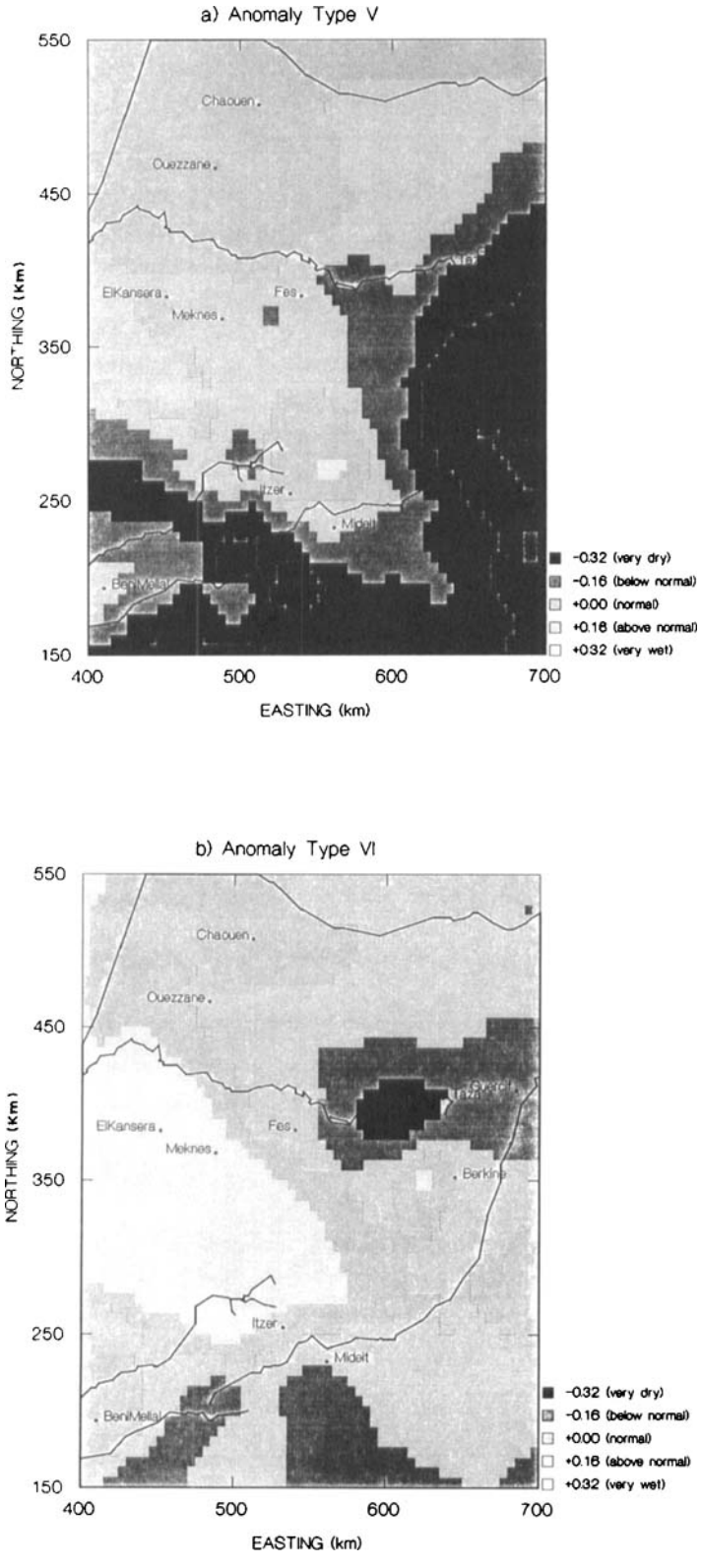

Figure 8. Anomaly types V and VI as defined by ordinary block kriging. See Fig. 4 for explanation

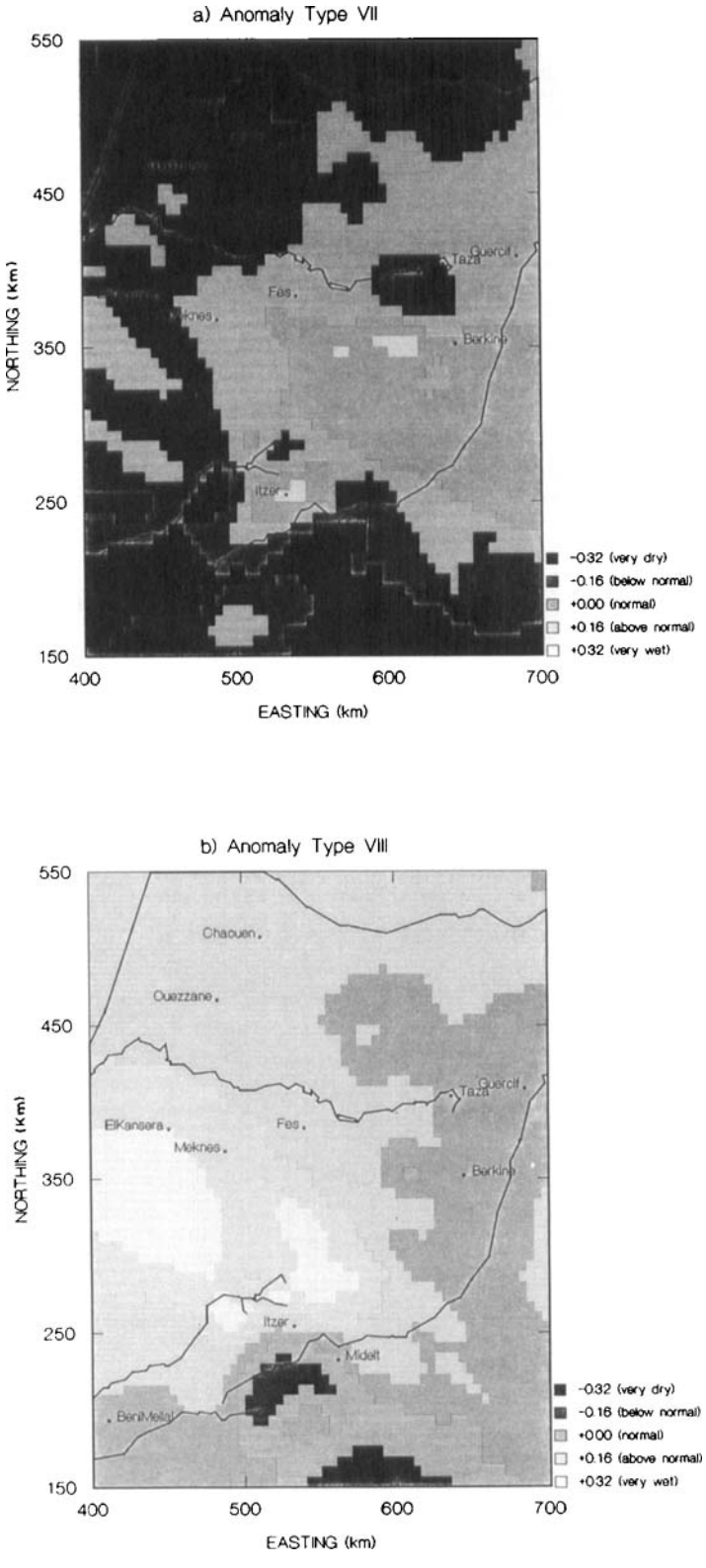

Figure 9. Anomaly types VII and VIII as defined by ordinary block kriging. See Fig. 4 for explanation

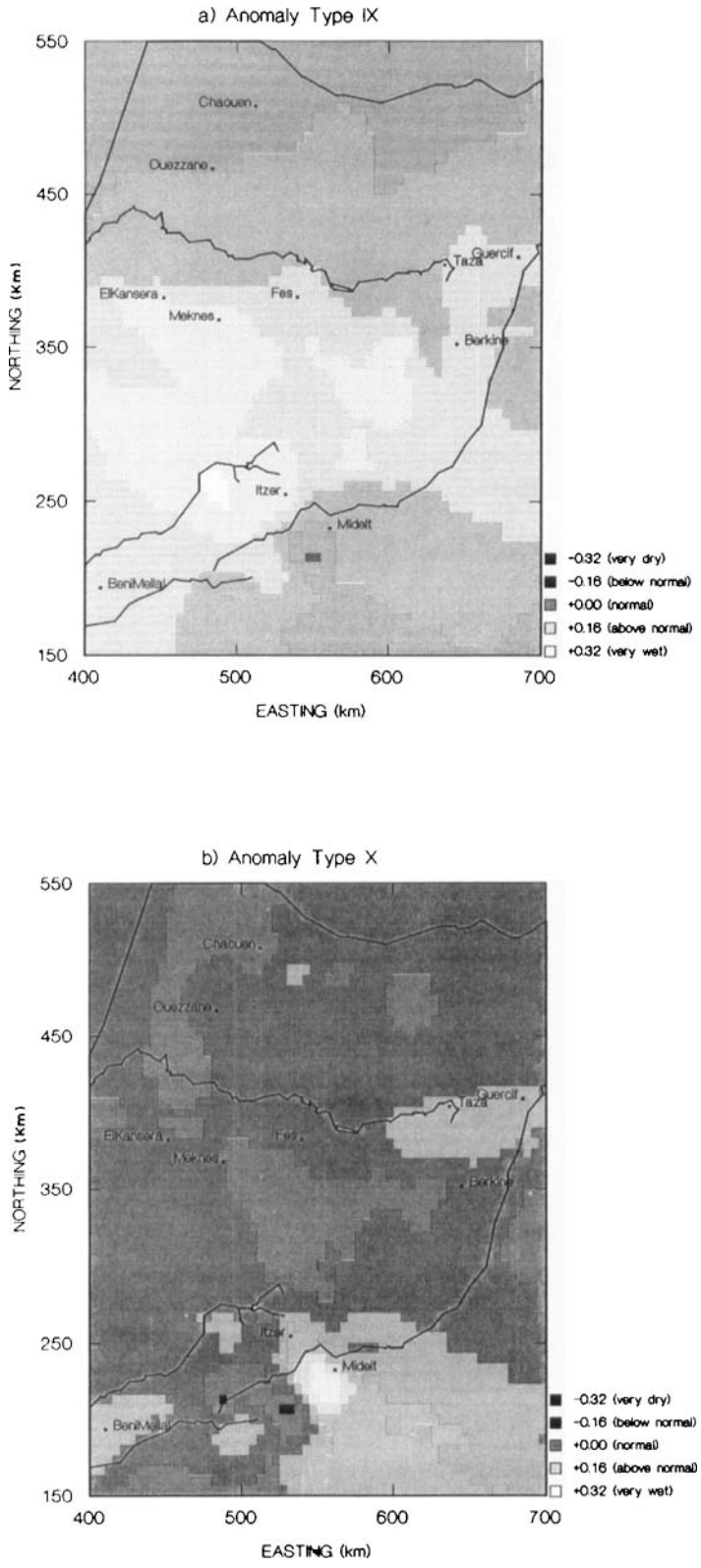

Figure 10. Anomaly types IX and X given by ordinary block kriging. See Fig. 4 for explanation

Anomaly type X

This types corresponds to a mild extended drought that spares only the south-east (Figure 10(b)). The anomaly may be related once again to a high frequency of the Mauritanian perturbation affecting the oriental side of the High Atlas. In this case, the local cyclogenesis centres are shifted to the other side of the mountains. This type of circulation dominated in the 1910s and the late 1960s (Figure 6).

CONCLUSIONS

The anomaly types identified can be classified as wet, dry, and normal, showing a mixture of deficits and excesses. They show varying degrees of structured variability. Severe and widespread droughts have very similar variograms, especially types II, VII, and X. The range of the spherical schemes are shortest for the dry patterns, suggesting a pure nugget effect due to the high degree of homogeneity over the area of study. Greatest ranges are associated with wet patterns. The quality of fit of the models is variable and suffers from the spatial distribution of the sample sites. Ordinary block kriging was utilized over the area of study to derive and distinguish the various anomaly types. The kriging variances are almost identical for the 10 types, with the highest values associated with noisy structures and remote regions of the Gharb, north-west and south-east corners.

Some of the anomaly types form a positive–negative image of given atmospheric circulation patterns. This is the case for types I and IV, and types II and IX. The first pair corresponds to either an extended excess or extended deficit linked to the relative position of the storm tracks with respect to Morocco. The second pair may be due to local cyclogenesis centred either in the Atlantic region (type IX) or south of the High Atlas (type II).

Other associations represent varying degrees of strength of a single atmospheric anomaly. This is the case for types VI and VIII, and types III and X.

The postulated atmospheric circulation anomalies associated with the spatio-temporal patterns of tree growth are based on three factors:

(i) The relative strength and position of the Azores High;
(ii) The importance and location of the local cyclogenesis centers;
(iii) The importance of the Mediterranean moisture input through north-eastern perturbations.

Temporal behaviour of the patterns revealed two dry episodes and two wet ones.

(i) The period 1860–1900 is basically dry. Anomaly types IV, V and VI predominate during the period. Negative association is indicated with the types I and III, which are wet anomalies.
(ii) The period 1925–1950 is also dry, as judged by the positive associations with types V and VI and the negative associations with the types I and III.
(iii) The period 1900–1920 was above average (or wet), being always in opposition to the 1860–1900 period.
(iv) The period 1950–1970 was also favourable (or wet).
(v) Although the 1970s do not cover 20 to 25 years to be identified as an episode the drought tendency of that decade, when types vi, vii, and ix were prevalent, should be noted.

The temporal clustering of the anomalies is striking and is similar to that Oladipo (1985) found in North America.

These four periods show a clear alternation in time for most of the anomaly types except types II and IX, which became established after 1940. The latter anomalies may be related to a recent change related to atmospheric forcing or may simply have a longer return period than that covered by the period of analysis.

It is noteworthy to mention that tree-ring data are less responsive to wetness, because the limiting factor varies between trees at the same site and also between sites in a given region. Slight or significant wetness anomalies would allow trees to grow to their maximum potential set by their age, stand density, and characteristics or genetic heritage. In this case the indication of wetness is obscure and may even be misleading. With a moisture deficit, all trees are subject to the same limiting factor and their response is unambiguous. Nevertheless, the results show that wetness anomalies are real because they are negatively

associated with dry anomalies. They are also correctly associated with the well-known wet episode of the 1900–1920.

These results present a first explanation of the patterns of drought attributes. The drought-prone area of the Middle Atlas experiences drought frequently even when the rest of the country is experiencing normal to above normal moisture conditions. The analysis could gain considerably from a detailed and quantitative analysis of the pressure types, which would help in the understanding of the dynamics of climate over Morocco and pinpoint the forcing mechanisms responsible for them. Similarly, it would be interesting to extend the period of analysis using an equivalent sample density. The results indicate that tree-ring data have great potential for reconstructing pressure anomalies over Morocco, which can be of great benefit through the prediction possibilities of the North Atlantic Oscillation.

ACKNOWLEDGEMENTS

We would like to thank the IAV-USAID University of Minnesota project for their support. Many thanks also to the reviewers for their comments.

REFERENCES

Blasing, T. J. 1975. *Methods for analyzing climatic variations in the North Pacific Sector and western North America for the last few centuries.* PhD dissertation, University of Wisconsin, Madison.

Chbouki, N. 1992. *Spatio-temporal characteristics of drought as inferred from tree-ring data in Morocco.* PhD dissertation, University of Arizona, Tucson, AZ.

Clark, I. 1979. *Practical Geostatistics*, Applied Science Publishers, Essex, 129 pp.

Cook, E. R. 1987. 'The decomposition of tree-ring series for environmental studies', *Tree-ring Bull.*, **47**, 37–59.

Delhomme, J. P. 1976. *Application de la théorie des variables régionalisées dans les sciences de l'eau.* Docteur-Ingénieur Thesis, Paris School of Mines.

Direction de la Météorologie Nationale 1990. *Les types de temps au Maroc*, Casablanca.

EPA 1988. *Geo-EAS: Geostatistical Environmental Assessment Software. Reference Manual*, Environmental Protection Agency, Environmental Monitoring Systems Laboratory, Las Vegas, NV.

Fritts, H. C. 1976. *Tree Rings and Climate*, Academic Press, London, 567 pp.

Greenacre, M. 1984. *Theory and Applications of Correspondence Analysis*, Academic Press.

Holmes, R. L., Adams, R. K. and Fritts, H. C. 1986. *Tree-ring Chronologies of Western North America: California, Eastern Oregon and Northern Great Basin with Procedures Used in the Chronology Development Work including Users Manuals for Computer Programs COFECHA and ARSTAN*, Laboratory of Tree-ring Research, Tucson, AZ.

Isaaks, H. E. and Srivastava, R. M. 1989. *An Introduction to Applied Geostatistics*, Oxford University Press, Oxford, 561 pp.

Johnson, R. A. and Wichern, D. W. 1988. *Applied Multivariate Statistical Analysis*, Prentice Hall, NJ, 607 pp.

Journel, A. G. and Huijbregts, C. 1978. *Mining Geostatistics*, Academic Press, 600 pp.

Legendre, L. and Legendre, P. 1984. *Ecologie Numérique*, Vols I and II, 2nd edn, Masson and the Quebec University Press, Quebec, 419 pp.

Matheron, G. 1971. *The Theory of Regionalized Variables and its Applications*, Cahier No 5, Centre de Morphologie Mathematique de Fontainbleau, 211 pp.

Meko, D. M. 1988. 'Temporal and spatial variation of drought in Morocco', in *Proceedings, Drought, Water Management and Food Production*, Agadir, Morocco, 21–24 November 1985. Imprimerie de Fedala, Mohammedia, 55–82.

Myers, D. E. 1991. 'On variogram estimation', in *The Frontiers of Statistical Scientific Theory and Industrial Applications*, Volume II of the Proceedings of ICOSCO-I, The first International Conf. on Statistical Computing, Cesme, Turkey, 30 Mar–2 April, 1987 American Sciences Press, pp. 261–281.

Oladipo, E. O. 1985. 'Spatial patterns of drought in the interior plains of North America', *J. Climatol.*, **16**, 495–513.

Rouhani, S. and Hall, T. J. 1989. 'Space-time kriging of groundwater data', in Armstrong, M. (ed), *Geostatistics*, Vol. II, Kluwer, Dordrecht, pp. 639–651.

Rouhani, S. and Myers, D. E. 1990. 'Problems in space-time kriging of geohydrological data', *Math. Geol.*, **22** (5), 611–623.

Stockton, C. W. 1988. 'Current research progress toward understanding drought', in *Proceedings, Drought, Water Management and Food Production*, Agadir, Morocco, 21–24 November 1985. Imprimerie de Fedala, Mohammedia, 21–35.

Stokes, M. A. and Smiley, T. L. 1968. *An Introduction to Tree-ring Dating.* University of Chicago Press, Chicago, 73 pp.

Till, C. 1985. *Recherches dendrochronologiques sur le Cèdre de l'Atlas (Cedrus atlantica (Endl.) Carriere.) au Maroc.* Phd thesis, U.C.L. Louvain-La-Neuve, Belgium.